Frustration-Driven Successive Metamagnetic Transitions in TbB_4

T. Inami,[1] K. Ohwada,[1] Y. H. Matsuda,[2] Z. W. Ouyang,[2]
H. Nojiri,[2] D. Okuyama,[3] T. Matsumura,[3] and Y. Murakami[3]

[1] *Synchrotron Radiation Research Unit, Japan Atomic Energy Agency, Sayo, Hyogo 679-5148, Japan*
[2] *Institute for Materials Research, Tohoku University, 2-1-1 Katahira, Sendai 980-8577, Japan*
[3] *Department of Physics, Faculty of Science, Tohoku University, Aoba, Sendai 980-8578, Japan*

(Dated: August 21, 2008)

Resonant magnetic x-ray diffraction experiments on the Shastry-Sutherland lattice TbB_4 were carried out under strong pulsed magnetic fields up to 30 T. TbB_4 exhibits a multi-step magnetization process above 16 T when magnetic fields are applied along the *c*-axis. We examined the intensity of the 010 magnetic reflection as a function of magnetic field and found that the magnetization plateau phases are accompanied by large XY components of magnetic moments, in contrast to normal fractional magnetization plateau phases. The magnetization was calculated using a simple spin model deduced from the above result. Finally we propose that frustration is the key to understanding the observed multi-step magnetization.

PACS numbers: 75.25.+z,75.30.Kz,78.70.Ck

When one applies pressure to a substance, the volume will be reduced at all times depending on its compressibility. In contrast to such natural behavior, several magnetic materials exhibit magnetization plateaus, where the magnetization keeps a constant value at a finite range of magnetic fields even below the saturation field. This "zero compressibility" is simply ascribed to the fact that S_z is a good quantum number, while a variety of mechanisms give rise to plateaus in the magnetization curve.

Let us consider only plateau phases in ordered states here. The easy-axis magnetization of an Ising antiferromagnet is most comprehensible. An example is the one-third magnetization plateau of $CoCl_2{\cdot}2H_2O$ [1]. Competing exchange interactions stabilize the ↑↑↓ structure just below the saturation field. The multi-step magnetization curves of $PrCo_2Si_2$ [2] and CeSb [3] are also classified into this category. The plateau phases are described by a complex sequence of up- and down-spins.

Magnetization plateaus are also observed in Heisenberg spins. In geometrically frustrated Heisenberg antiferromagnets, one-third (↑↑↓) and one-half (↑↑↑↓) plateaus are sometimes observed in triangular- and tetrahedon-based lattices, respectively. Although the field range of the plateau phase is zero for these lattices if only the nearest-neighbor interaction is taken into account, additional mechanisms, such as a four-spin exchange coupling, quantum fluctuations, single-ion anisotropy and magnetoelastic couplings, stabilize the plateau phase in real magnets [4, 5, 6, 7]. A crucial point is that all plateau phases have a collinear magnetic structure. No ordered magnetic moment perpendicular to the magnetic field exists in the plateau phases.

Recently, a multi-step magnetization curve was observed in TbB_4. Intriguingly, several experimental evidences indicate that TbB_4 resembles none of the above-mentioned magnets. In this letter, we report on resonant x-ray diffraction (RXD) experiments on TbB_4 up to 30 T. The field dependence of the magnetic intensity provided decisive information on the magnetic structure of the field-induced phases. From this result, we show that TbB_4 indeed belongs to a rare class of magnets, characterized by ordered perpendicular components in the plateau phases. We also show that frustration plays a vital role in the multi-step magnetization process on the basis of the calculation of magnetization curves.

The rare-earth tetra-boride RB_4 crystallizes into a tetragonal structure (space group: $P4/mbm$). The network of the rare-earth ions is equivalent to the frustrated Shastry-Sutherland (SS) lattice [8]. Several pieces of work have thus been carried out from a viewpoint of frustration between rare-earth quadrupole moments [9, 10]. Somewhat confusingly, in the strict sense, classical continuous spins on the SS lattice are not frustrated, because the ground state is a unique helical or Néel structure and has no degeneracy [8]. However, for helical structures, none of the antiferromagnetic bonds are antiparallel and thus local pair exchange-energy is not minimized. The spins are not satisfied and still feel "frustration". We will revisit this point later.

In TbB_4, there are two transition points T_{N1}=44 K and T_{N2}=22 K. The total angular momentum of the Tb ion is large (J=6) and hence the Tb spin is approximated by a classical spin. The magnetic structure between T_{N1} and T_{N2} revealed by neutron powder diffraction experiments is shown in Fig. 1(a) [11]. The magnetic moments are XY-type and are confined in the basal *ab*-plane. Additional in-plane anisotropy orients the moments parallel to the diagonal line. The nearest-neighbor interaction J_1 is antiferromagnetic. The next-nearest-neighbor interaction J_2 is probably antiferromagnetic, and J_1 and J_2 form a frustrated SS lattice. In RB_4, the further-neighbor antiferromagnetic interaction J_3 is taken into account, which stabilizes the observed magnetic structure. In this structure, the J_2 bond is not satisfied. Below T_{N2}, the mag-

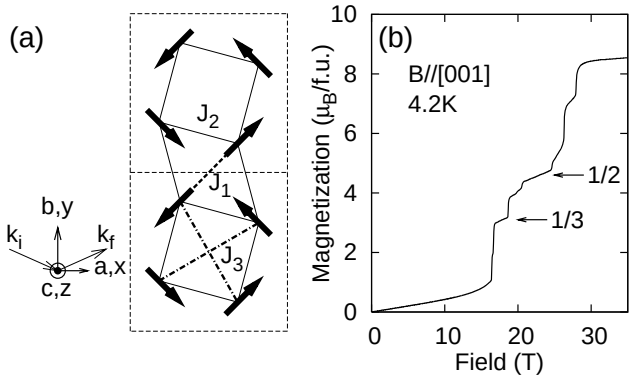

FIG. 1: (a) Magnetic structure of TbB_4 between T_{N1} and T_{N2}. A large square is the unit cell. Major interactions (J_1 : broken line, J_2 : solid line, J_3 : dot-dashed line) are shown. Sample coordination (a, b, c, x, y and z) and incident and scattered x-rays (k_i and k_f) are also shown. (b) Magnetization process of TbB_4 taken from Ref. [13].

netic moments rotate in the ab-plane and a collinear-like antiferromagnetic structure is realized. This transition is considered to be a ferro-quadrupole order [12] and is destroyed by application of magnetic fields.

The magnetization process of TbB_4 parallel to the c-axis shown in Fig. 1(b) exhibits multi-step metamagnetic behavior between 16 and 28 T [13]. The number of the steps is reported to be nine, and the one-half magnetization plateau is most prominent. When a magnetic field is applied parallel to the [100] and [110] directions, a single metamagentic transition is observed. Magnetization measurements of diluted samples indicated that the multi-step magnetization is inherent to the phase between T_{N1} and T_{N2} [14]. The metamagnetic behavior suggests that the essential nature of the transitions is level-crossing between low-lying multiplets [15]. However, the origin of the multiple successive transitions is not easily understood. Magnetic structures in the high-field plateau phases provide useful information, thus we conducted an x-ray diffraction experiment under strong pulsed magnetic fields, which has been recently developed utilizing brilliant third-generation synchrotron x-rays [16, 17, 18]. Although magnetic x-ray scattering cross-sections are very small, we utilized resonant enhancement of magnetic scattering [19].

Synchrotron x-ray diffraction experiments were carried out at undulator beamline BL22XU at SPring-8. The x-ray energy was tuned to the Tb L_{III} absorption edge (7.514 keV). Magnetic fields up to 30 T were generated using a small pulsed magnet (20 mm in outer diameter and 24 mm in length). The pulse duration was about 0.6 ms. The magnet was a split-pair, and two windows were prepared for incoming and outgoing x-rays. The magnet and a sample were attached to the 100 K and 10 K stages of a conventional closed cycle refrigerator, respectively. Details of experimental setup are described in Ref. [16]. Single crystals of TbB_4 were grown by the floating zone method. The sample was a thick plate of dimensions 1 mm×1 mm×0.5 mm with a polished (010) surface. The FWHM of the ω profile of the 020 reflection was about 0.06°.

The scattering plane was horizontal. The b^* axis lay in the scattering plane and the c-axis was perpendicular to the scattering plane. We observed the forbidden 010 reflection, which is a magnetic Bragg point as demonstrated in the neutron experiment [11]. The azimuthal angle Ψ, which is the rotation about the scattering vector, is a key parameter in RXD. We define Ψ=0 when the c-axis is perpendicular to the scattering plane. Ψ was kept close to zero throughout this experiment. Magnetic fields were applied parallel to the c-axis. We used a high-counting-rate detector and measured diffraction intensity as a function of time with a typical resolution of 10 μs. The field strength was also monitored as a function of time, and we obtained the field dependence of the diffraction intensity from these two series of data. Polarization of scattered x-rays were separated using a PG (006) crystal analyzer. In order to prevent the sample from being heated by x-ray irradiation, we inserted a chopper into incident x-rays. The window width was about 2 ms and the duty cycle was about 0.01.

In Fig. 2(a), we show the peak intensity of the 010 reflection as a function of photon energy below T_{N2} and above T_{N1}. The fluorescence spectrum is also shown. The intensity of the 010 reflection exhibits huge enhancement at the L_3 main edge, implying that the resonance is ascribed to electric dipole (E1) transition. Subsequent measurements were carried out at the peak energy (7.512 keV). The temperature dependence of the integrated intensity of the 010 reflection is shown in Fig. 2(b). The intensity appears below T_{N1} and is constant below T_{N2}. The effect of beam heating is estimated to be at most 2 K from the differences between the reported and observed transition temperatures.

Here we briefly mention the resonant x-ray scattering amplitude [21] of the Tb ion, which is proportional to

$$f_{\rm res} \propto iC_1(\boldsymbol{\epsilon}_{\rm f}^* \times \boldsymbol{\epsilon}_{\rm i}) \cdot \boldsymbol{m} + C_2\, \boldsymbol{\epsilon}_{\rm f}^\dagger\, O\, \boldsymbol{\epsilon}_{\rm i}, \qquad (1)$$

where $\boldsymbol{m}$ is the magnetic moment and $\boldsymbol{\epsilon}_{\rm i}$ and $\boldsymbol{\epsilon}_{\rm f}$ are the polarization vectors of the incident and scattered x-rays, respectively. The symmetric second-rank tensor O describes anisotropy of the Tb 5d orbital caused by anisotropic crystal environment or quadrupole order and is represented by a linear combination of the five elements O_{xy}, O_{yz}, O_{zx}, O_{22} and O_{20}. The first term in eq.(1) is magnetic scattering and the last term causes anisotropy of the tensor of susceptibility (ATS) scattering. Thorough measurements on temperature and azimuthal angle dependence with polarization analysis were performed by TM [20]. The results were consistent with the magnetic

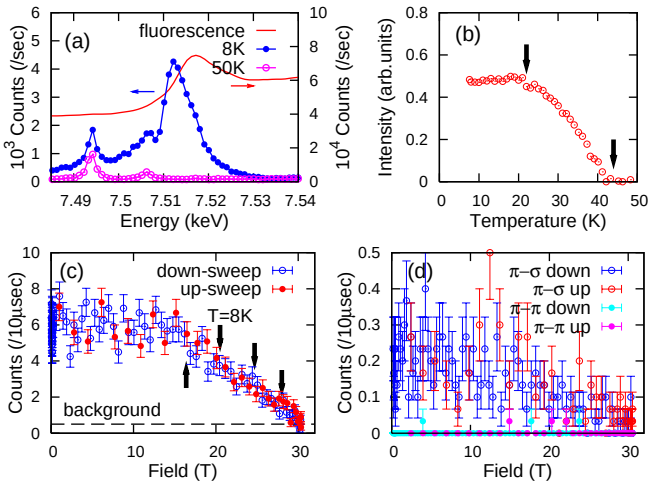

FIG. 2: (color online) (a) Peak intensity of the 010 reflection as a function of photon energy below T_{N2} and above T_{N1}. Huge enhancement is evident at the L_3 edge of the fluorescence spectrum. Small peaks observed at 50 K are multiple scattering. (b) Intensity of the 010 reflection as a function of temperature. Arrows indicate T_{N1}=44 K and T_{N2}=22 K. The sample temperature is higher than the thermometer by 2 K because of beam heating. (c) Field dependence of the peak intensity of the 010 reflection at 8 K. The arrows indicate the onset of the high-field phases (16.4 T), the lower and upper critical fields of the one-half plateau phase (20.5 T and 24.7 T) and the saturation field (28 T) at 4 K. (d) Field dependence of the 010 reflection at 8∼10 K. Polarization of scattered x-rays are separated. Red and blue (magenta and cyan) circles are up- and down-sweeps of the π-σ (π-π) channel.

structure obtained in the neutron experiment [11], and it was confirmed that $0k0$ reflections (k : odd integer) at Ψ=0 are magnetic scattering.

The field dependence of the peak intensity of the 010 reflection at 8 K is shown in Fig. 2(c). The data were averaged over 12 field-scans. The intensity is constant up to 16 T and gradually decreases above 16 T as the field is increased. An important outcome is that a considerable amount of the intensity remains in the magnetization plateau phases above 16 T. From this result, we understand that the plateau phases include (0,1,0) modulated magnetic moments and/or anisotropic 5d orbitals.

The second important outcome is obtained from polarization dependence of scattered x-rays. States of linear polarization are labeled by σ and π when they are normal and parallel to the scattering plane, respectively. The incident polarization was π. The scattering amplitudes $f_{\rm res}(\theta)$ of $\pi\pi'$ and $\pi\sigma'$ channels for each magnetic and ATS component at Ψ=0 are listed in Table I, where θ is the Bragg angle. The structure factor $f_{\rm res}(\theta)\sum_{\rm i} e^{i2\pi \boldsymbol{K}\boldsymbol{R}_{\rm i}}$ at (0,k,0) is proportional to either $if_{\rm res}(\theta)\sin 2\pi k\delta$ or $f_{\rm res}(\theta)\cos 2\pi k\delta$, where the fractional coordinate of the Tb site $\delta \sim 0.317$. The structure factor below 16 T is proportional to $m_x \cos\theta \sin 2\pi k\delta$. In Fig. 2(d), field dependence of $\pi\pi'$ and $\pi\sigma'$ channels of the 010 reflection

	m_x	m_y	m_z	O_{xy}	O_{yz}	O_{zx}	O_{22}	O_{20}
$\pi\pi'$	0	0	$i\sin 2\theta$	0	0	0	-1	$-\cos 2\theta$
$\pi\sigma'$	$i\cos\theta$	$-i\sin\theta$	0	0	$\cos\theta$	$\sin\theta$	0	0

TABLE I: Scattering amplitude of each component of magnetic and ATS scattering at Ψ=0 for $\pi\pi'$ and $\pi\sigma'$ channels.

are shown. The data were averaged over 30 field-scans. It is obvious that the scattered x-rays are dominated by $\pi\sigma'$ channel at all field ranges. Hence it is inferred from Table I that the scattering intensity of the 010 reflection arises from m_x+m_y or O_{yz}+O_{zx}. We also observed the 050 reflection (not shown) without the analyzer. In spite of large difference in θ (6.6° and 35.2°), the field dependence of the 050 reflection is very similar to that of the 010 reflection. This fact indicates that the intensities of both the zero- and high-field phases are proportional to $\cos\theta \sin 2\pi k\delta$ and that m_z ($\propto \sin 2\theta$) does not exist in the high-field phases. In addition, recent neutron diffraction experiments of TbB_4 under pulsed magnetic fields have shown that the field dependence of the 010 reflection in neutron diffraction is also similar to that of x-ray diffraction [22]. Neutrons observe m_x, m_y and m_z. Hence pure O_{yz}+O_{zx} order is inconsistent with the neutron result. m_x or m_y must exists. Actually all data are well interpreted by assuming that the major order parameter in the high-field phases is m_x, magnetic moments perpendicular to magnetic fields.

This is a rather surprising result, because all magnetic moments in plateau phases are parallel or antiparallel to the magnetic field as mentioned in the introduction. A canted magnetic structure, usually derived from the coexistence of parallel and perpendicular components, results in a continuous magnetization curve unlike the observed step-like magnetization process. Accordingly, we submit an idea that in TbB_4 the magnetic structures in the plateau phases consist of very hard XY-type magnetic moments and Ising-like magnetic moments.

In order to interpret this novel magnetic structure, we propose the following spin model. The low-lying multiplets are approximated by the ground-state XY-spin $\vec{S}$ with the in-plane anisotropy E and the excited-state Ising spin $\vec{s}$ with the energy gap G. The spin Hamiltonian is

$$H = \sum_{m=1,2,3} J_m \left(\sum_{i,j} \left(S_i^x S_j^x + S_i^y S_j^y \right) + \sum_{k,l} s_k^z s_l^z \right) - E \sum_i (|S_i^x S_i^y| - \frac{1}{2}) + G \sum_k (s_k^z)^2 - g\mu_{\rm B} H_z \sum_k s_k^z,$$

where the spins are unit vectors, i and j sites are occupied by XY spins and k and l sites are occupied by Ising spins.

Magnetization curves were calculated for finite-size cells with periodic boundary conditions. We consider 4 spins in the crystallographic unit cell (1 × 1 cell). For simplicity, we initially consider a four-clock model by

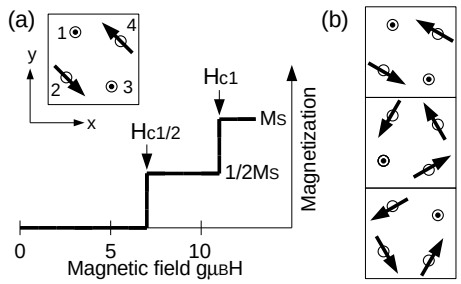

FIG. 3: (a) Calculated magnetization curve for $E \to \infty$. The magnetic structure of the one-half plateau phase is shown in the inset. $\odot$ denotes a spin parallel to the z-axis. (b) Possible magnetic structure of the one-third plateau phases.

taking the limit $E \to \infty$. For example (see Fig. 3(a)), allowed states for spins 1 and 3 are $\swarrow$ $(-\frac{\sqrt{2}}{2}, -\frac{\sqrt{2}}{2}, 0)$, $\nearrow$ $(\frac{\sqrt{2}}{2}, \frac{\sqrt{2}}{2}, 0)$, $\odot(0,0,1)$ and $\otimes(0,0,-1)$. In this case, we calculated energies of all 4^4=256 states and found ground states. For rather wide parameter sets, this model has the same ground state as observed. A calculated magnetization curve for $J_1 = 2, J_2 = 1, J_3 = 2$ and $G = 1$ is shown in Fig. 3(a). The one-half magnetization plateau is clearly reproduced and the corresponding magnetic structure is shown in the inset. Similar results were obtained with other sets of parameters and different cell sizes (2×2 and 1×3 cells).

It is interesting to note that a number of states that have various magnetizations are degenerate at the critical fields $H_{c1/2}$ and H_{c1}. This is in fact an ordinary phenomenon observed in metamagnetic transitions. However, if this degeneracy is lifted, the multi-step magnetization curve of TbB_4 can be reproduced. Three mechanisms can lift the degeneracy: (i) difference in magnitude between S and s, (ii) interactions beyond J_3, and (iii) frustration. While the first two mechanisms cause symmetric splits at $H_{c1/2}$ and H_{c1}, the observed magnetization curve is asymmetric. For instance, the one-third plateau is clearly visible, whereas the two-third plateau is indistinguishable, as seen in Fig.1(b). It is evident that the last mechanism, frustration, plays an essential role. A possible magnetic structure of the one-third plateau phase is shown in Fig. 3(b). Here we set the in-plane anisotropy E finite so that the moments can rotate in the ab-plane. The Ising sites behave like defects. In frustrated magnets, as pointed out in the introduction, the local pair exchange-energy is not minimized. Hence, when a defect is introduced, the magnetic structure around the defect relaxes and gains exchange energy. This does not happen in magnetic lattices without frustration, because all exchange energies have been minimized.

For magnetic systems with short-range interactions, it is expected that small commensurate unit cells are more stable than large or incommensurate cells. Thus it is plausible that a finite number of selected magnetization steps appear in the magnetization curve through the frustration mechanism. This mechanism is active only when the density of the Ising sites is less than half (up to J_3). Therefore the degeneracy is lifted only at $H_{c1/2}$. The diffraction intensity of magnetic structures based on the model shown in Fig. 3(a) is one-quarter of the intensity at 0 T. The observed intensity is, however, about 40% of that at 0 T, implying presence of other order parameters, such as O_{20} and O_{yz}.

In conclusion, we have investigated the multi-step magnetization process of TbB_4 using RXD. The magnetic intensity observed in the plateau phases illustrates that large XY-components of the magnetic moments coexist with aligned Z-components. A simple spin model reproduces the one-half magnetization plateau, and it is found that the frustrated nature of the SS lattice lifts the degeneracy at the critical fields and creates the observed multi-step metamagnetic behavior. Paradoxically, frustration is not only an origin of degenerate states, but also breaks degeneracy.

This work was supported by Grant-in-Aid for Scientific Research on Priority Areas "High Field Spin Science in 100T" (No.451) from the Ministry of Education, Culture, Sports, Science and Technology (MEXT).

[1] H. Kobayashi and T. Haseda, J. Phys. Soc. Jpn. **19**, 765 (1964).
[2] T. Shigeoka et al., J. Phys. Soc. Jpn. **58**, 394 (1989).
[3] J. Rossat-Mignod et al., Phys. Rev. B **16**, 440 (1977).
[4] T. Sakakibara and M. Date, J. Phys. Soc. Jpn. **53**, 3599 (1984).
[5] L. E. Svistov et al., Phys. Rev. B. **67**, 094434 (2003).
[6] H. Kitazawa et al., Physica B **259-261**, 890 (1999).
[7] H. Ueda et al., Phys. Rev. Lett. **94**, 047202 (2005).
[8] B. S. Shastry and B. Sutherland, Physica B **108**, 1069 (1981).
[9] R. Watanuki et al., J. Phys. Soc. Jpn. **74**, 2169 (2005).
[10] D. Okuyama et al., J. Phys. Soc. Jpn. **74**, 2434 (2005).
[11] T. Matsumura et al., J. Phys. Soc. Jpn. **76**, 015001 (2007).
[12] T. Fujita et al., Abstr. Meet. Phys. Soc. Jpn. (63rd Annu. Meet., 2008), Part 3, 23aPS-86 [in Japanese] .
[13] S. Yoshii et al., J. Magn. Magn. Mater. **310**, 1282 (2007).
[14] F. Iga et al., private communications .
[15] Z. A. Kazeĭ et al., JETP Letters **84**, 441 (2006).
[16] Y. H. Matsuda et al., J. Phys. Soc. Jpn. **75**, 024710 (2006).
[17] Y. Narumi et al., J. Synch. Rad. **13**, 271 (2006).
[18] P. Frings et al., Rev. Sci. Instr. **77**, 063903 (2006).
[19] D. Gibbs et al., Phys. Rev. Lett. **61**, 1241 (1988).
[20] T. Matsumura et al., private communications .
[21] M. Blume, *Resonant Anomalous X-Ray Scattering* (Elsevier Science B.V., Amsterdam, 1994).
[22] S. Yoshii et al., private communications .